

Current Biology, Volume 27

Supplemental Information

**Coordination by Cdc42 of Actin, Contractility,
and Adhesion for Melanoblast Movement
in Mouse Skin**

Emma F. Woodham, Nikki R. Paul, Benjamin Tyrrell, Heather J. Spence, Karthic Swaminathan, Michelle R. Scribner, Evangelos Giampazolias, Ann Hedley, William Clark, Frieda Kage, Daniel J. Marston, Klaus M. Hahn, Stephen W.G. Tait, Lionel Larue, Cord H. Brakebusch, Robert H. Insall, and Laura M. Machesky

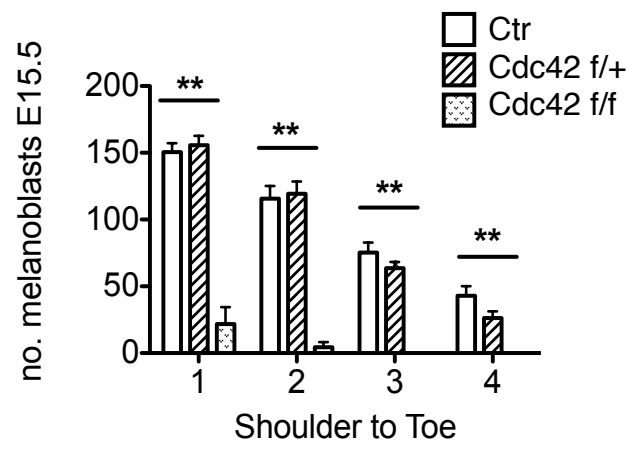
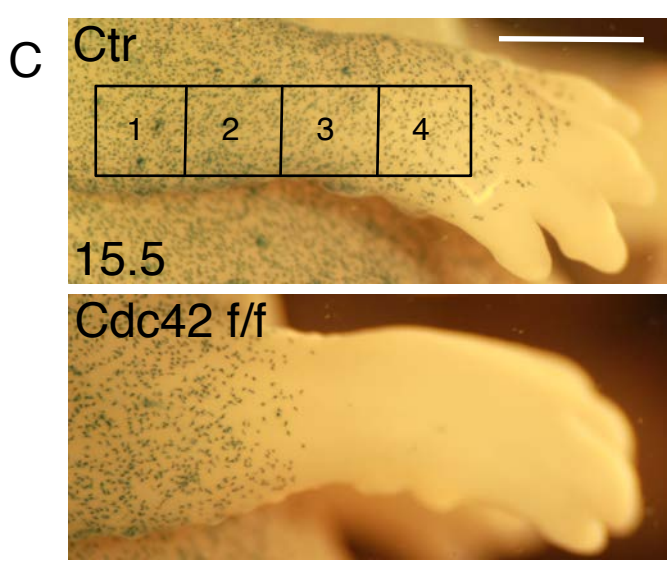
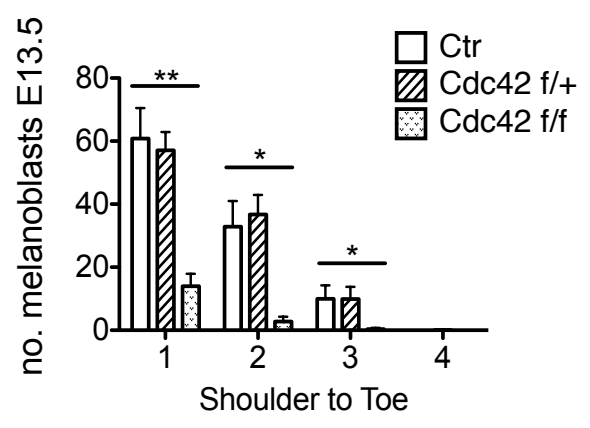
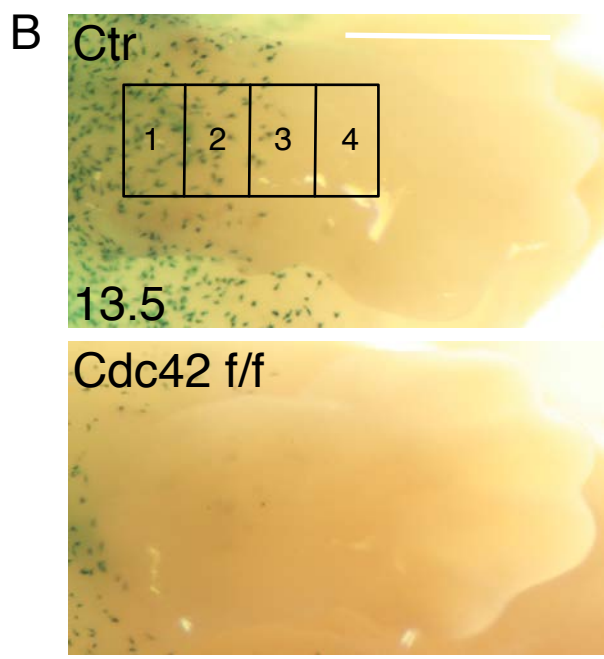


Figure S1

Figure S1- Deletion of RhoA from the melanocyte lineage does not change coat colour and Cdc42 null melanoblasts show a migration defect in the limbs (A) Images showing coat-colour, paw and tail of wild-type (Ctr) mice and RhoA f/f; Tyr::Cre mice at 6 weeks. (B) Forelimb of X-gal stained Ctr (Cdc42 wt/wt; DCT::LacZ) and Cdc42 f/f (Cdc42f/f; DCT::LacZ; Tyr::CreB+) embryos at E13.5. Scale 500 μ m and top images showing example grid used for quantification. Graph at left shows quantification of melanoblast number and positioning in E13.5 embryos where Ctr is Cdc42 wt/wt; DCT::LacZ and Cdc42 f/+ is Cdc42 f/+; DCT::LacZ; Tyr::CreB+ and Cdc42 f/f is Cdc42 f/f; DCT::LacZ; Tyr::CreB+. Quantification from at least 4 different embryos, 3 separate litters. Kruskal-Wallis one-way ANOVA test performed. Error bars show SEM. (C) Forelimb of β -galactosidase stained Control (Ctr) and Cdc42 f/f (as above) embryos at E15.5. Scale 1mm. Graph to the left shows melanoblast number and positioning (labels as described in B) in E15.5 embryos from at least 4 different embryos taken from 3 separate litters. Kruskal-Wallis one-way ANOVA test performed. Error bars show \pm SEM. *p<0.05, **p<0.01, n.s. not significant.
Linked to Figures 1-2

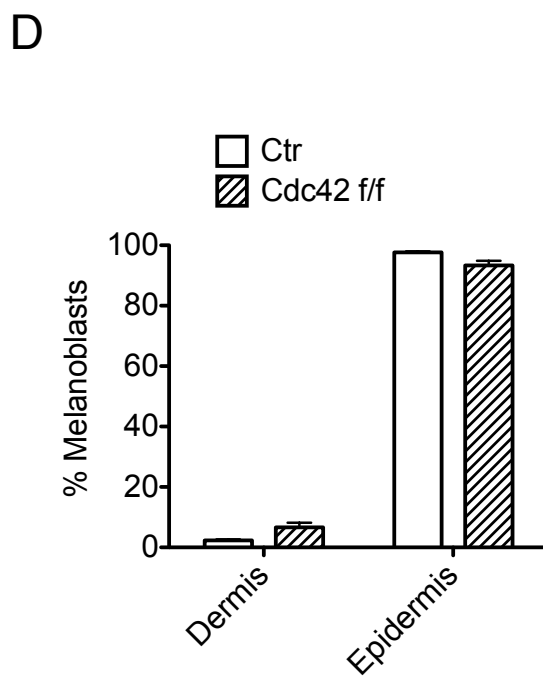
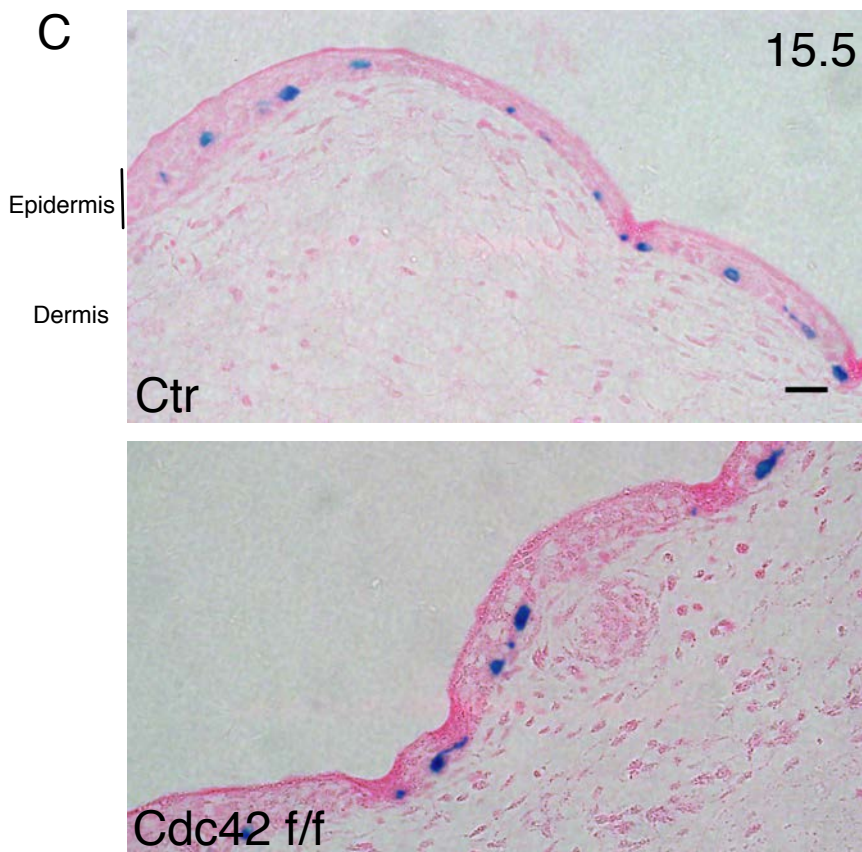
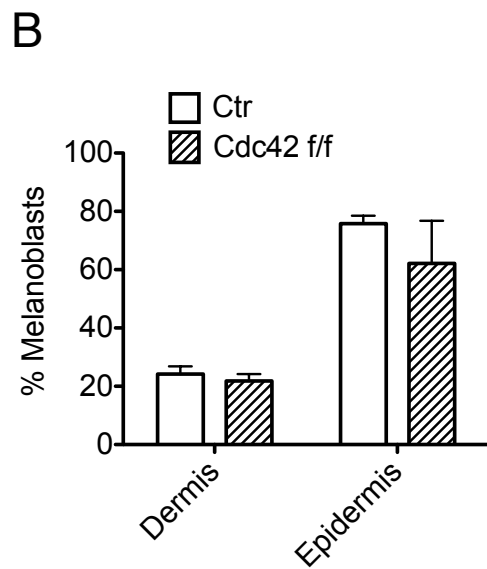
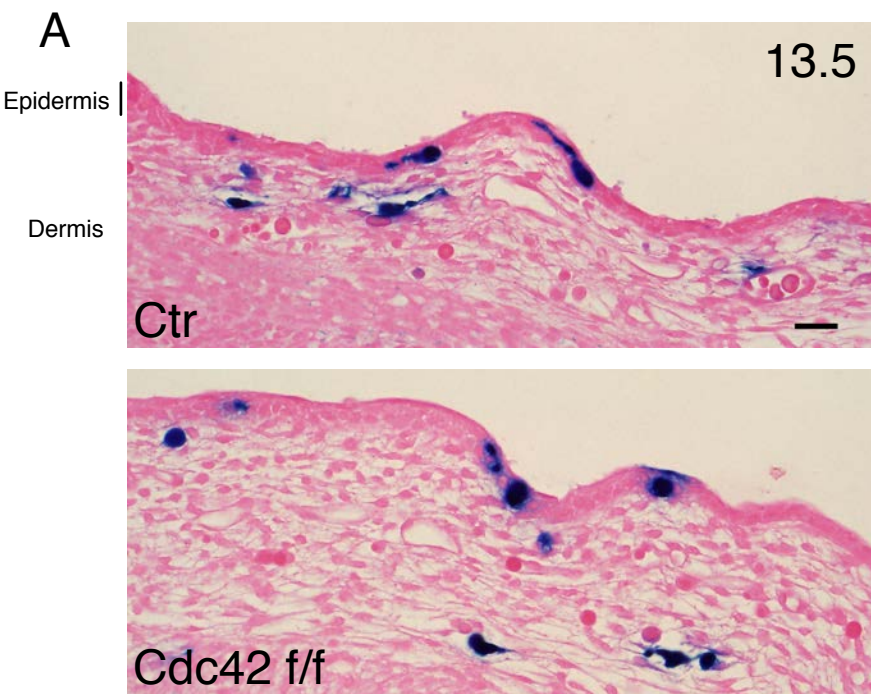


Figure S2- Cdc42 null melanoblasts cross from the dermis into the epidermis during development.

Images show X-gal stained Control Cdc42 wt/wt; DCT::LacZ (Ctr) and Cdc42 f/f; DCT::LacZ; Tyr::Cre (Cdc42 f/f) embryos counterstained with eosin. (A) Transverse sections from E13.5. (B) Quantification of melanoblasts in dermis and epidermis from Panel A from at least 5 different embryos from 3 different litters for each genotype, at least 85 cells per embryo. Error bars show SEM. Scale bar 10 μ m. (C) Transverse sections from E15.5. Scale 20 μ m. (D) Quantification of melanoblasts in dermis and epidermis from Panel C from at least 4 different embryos from 3 different litters for each genotype, at least 140 cells per embryo.

Linked to Figure 2

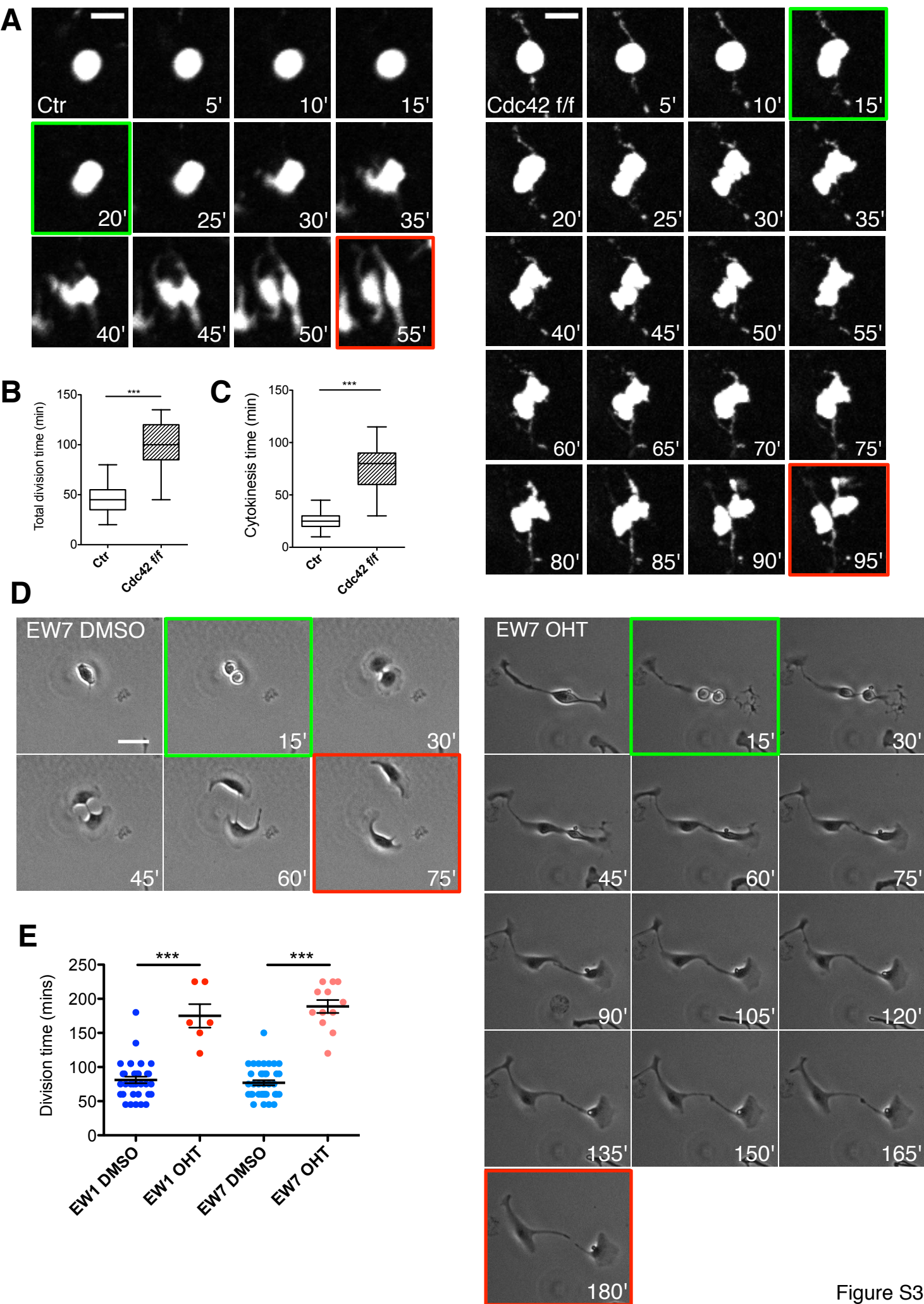


Figure S3

Figure S3- Cdc42 null melanoblasts show cytokinesis defects

(A) Stills from melanoblast division in Tyr::CreB⁺; Z/EG control (Ctr) and Cdc42 f/f Tyr::CreB⁺; Z/EG (Cdc42f/f) skin explants depicting rounding up, cleavage furrow formation (green) to separation of daughter cells (red). Images captured every 5min, Scale 10 μ m. See Movies 1-2. (B) Total division time from rounding up to complete separation of daughter cells (red). Measurements from at least 15 cells per genotype. (C) Cytokinesis time from cleavage furrow initiation (green) to separation of daughter cells (red). Measurements from at least 19 cells per genotype. (D) Time-lapse imaging of division of DMSO or OHT treated EW7 Cdc42 f/f; ROSA26::Cre-ER^{T2}; CDKN2^{-/-} melanocytes on fibronectin from rounding up, cleavage formation (green) to separation of daughter cells (red). Images captured every 15min, Scale 10 μ m. (E) Total division time from rounding up to complete separation of daughter cells. Box plots (B,C) show mean with maximum and minimum values. Graph (E) shows mean \pm SEM, ***p<0.001 t-test.

Linked to Figure 3 and Movies 1-2.

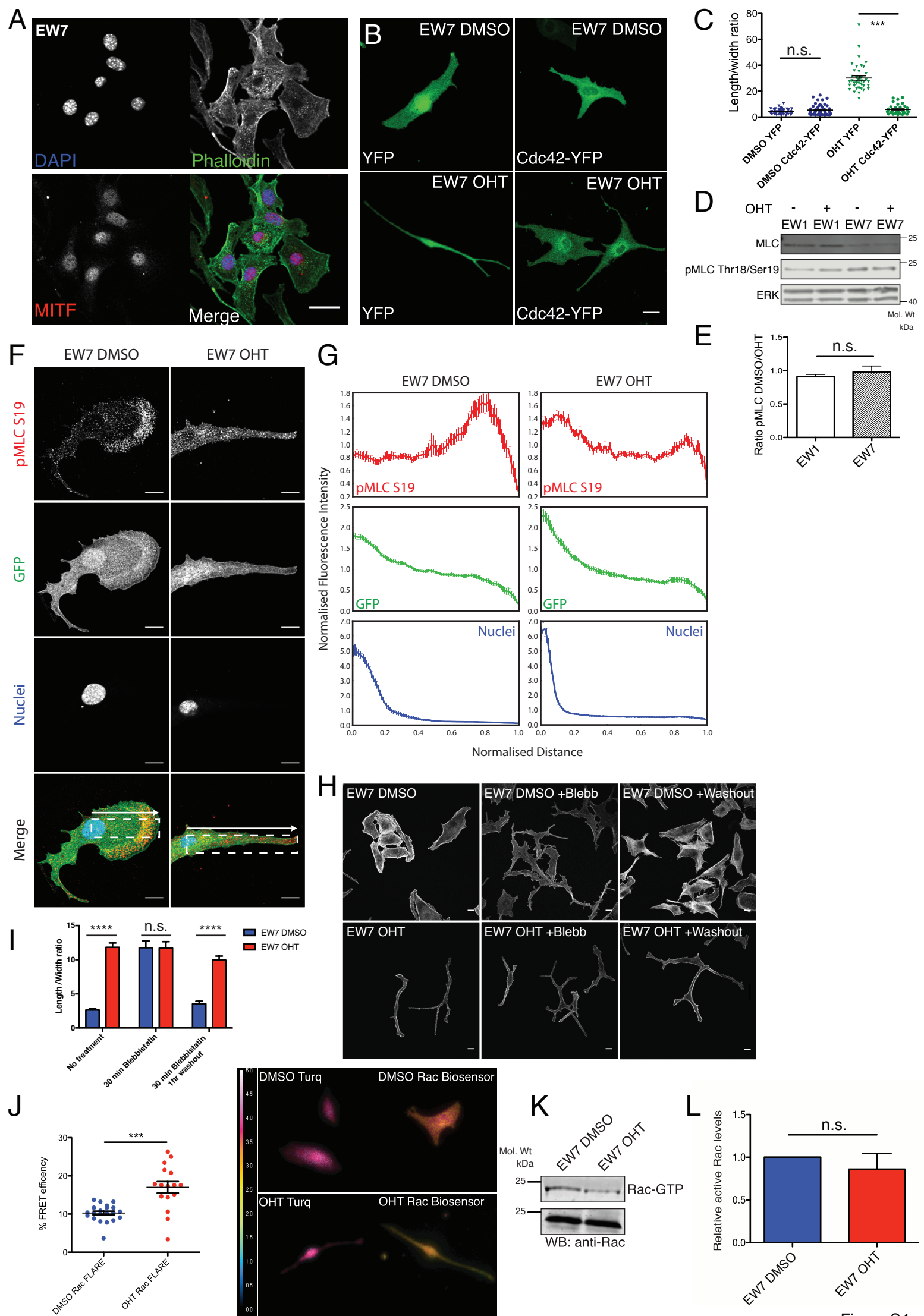


Figure S4

Figure S4- Cdc42 null melanocytes show mislocalised phospho-MLC but not reduced Rac1 activation

All panels show EW7 Cdc42 f/f; ROSA26::Cre-ER^{T2}; CDKN2^{-/-} melanocytes treated with DMSO (control) or OHT (to delete Cdc42). (A) EW7 melanocytes fixed and stained with DAPI (nucleus), phalloidin (F-actin) and MITF (melanocyte marker). Scale 20µm. (B) Images of DMSO (control) and OHT (Cdc42 deleted) EW7 melanocytes transfected transiently with YFP or Cdc42-YFP. Scale 20µm. (C) Quantification of length to width ratio of transfected melanocytes. (D) Western blot of total myosin light chain (MLC), phospho-MLC Thr18/Ser19, and ERK loading control in EW1 and EW7 melanocytes treated with DMSO or OHT. (E) Ratio of levels of p-MLC in DMSO/OHT treated cells. Average ratio taken from 3 Western blots. (F) Immunofluorescence imaging of EW7 DMSO and OHT-treated melanocytes, transfected with GFP, fixed and stained with DAPI (nuclei), and p-MLC antibody (Ser19 phospho- myosin light chain). Scale 10µm. White boxes show example areas 10µm tall used for quantification. (G) Quantified normalised fluorescence intensity profile of cells in Panel F from the centre of the nucleus to the leading edge of pMLC, GFP and DAPI staining in control and OHT-treated EW7 cells. N = 36-43 cells per condition over 3 experiments. (H) Control and OHT-treated EW7 cells incubated or not with Blebbistatin for 30min, or following 1 hour washout were fixed and stained with Alexa-Fluor 568-conjugated phalloidin. (I) Quantification of length to width ratio of cells in Panel G, N = 30 cells per condition over 3 experiments. (J) FRET efficiency of fluorophores in EW7 cells. N = 14-20 cells per condition. Heat maps showing lifetimes of control (dTurquoise) and Rac1FLARE.dc biosensor in EW7 cells. (K) Active Rac pulldown assay Western blot and (L) quantification of 4 independent experiments. Scale 10µm. Graphs show mean ± SEM, ***p<0.001, ****p<0.0001, n.s. not significant, t-test.

Linked to Figure 5

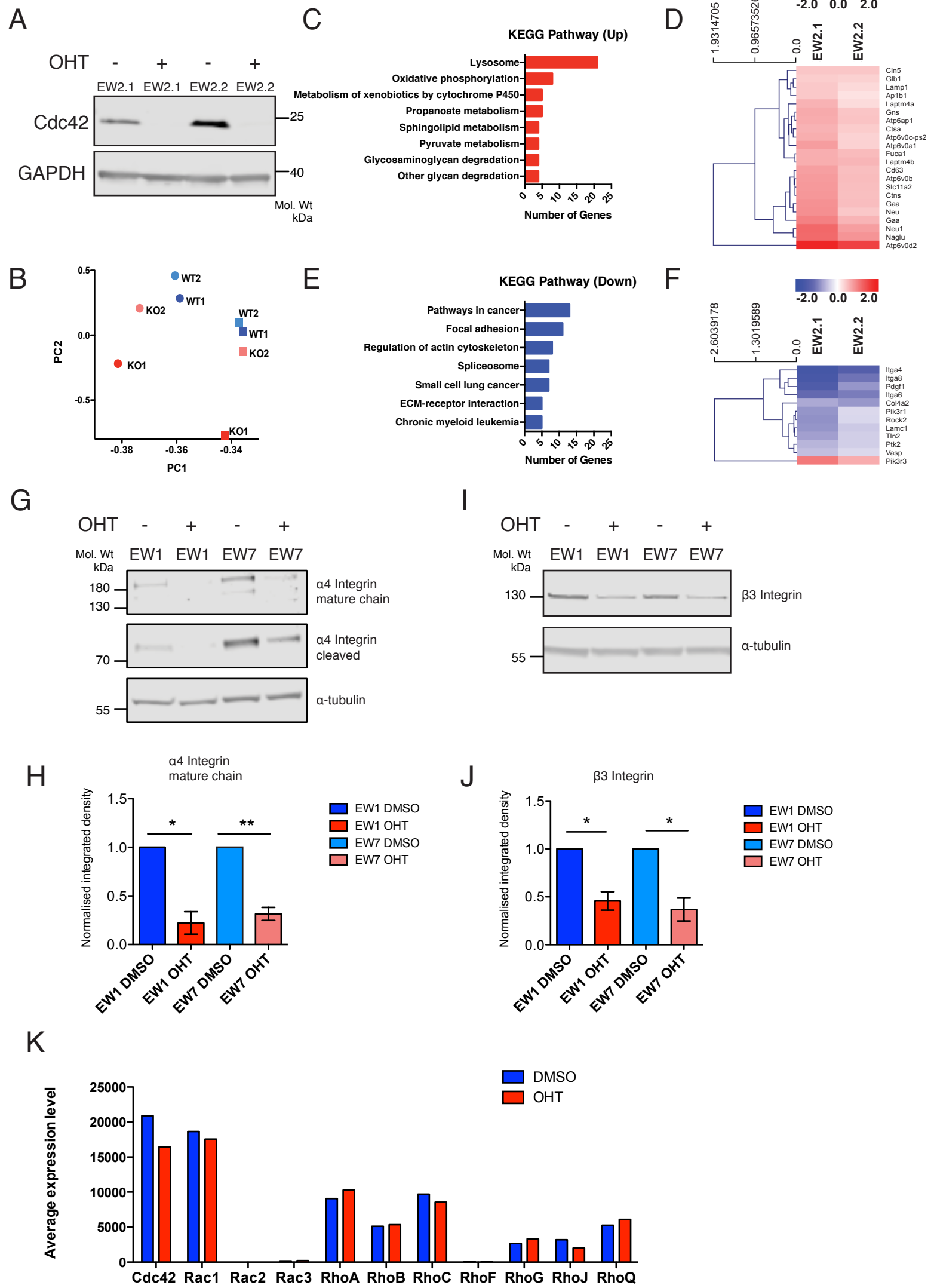


Figure S5, Woodham et al

Figure S5. Cdc42 null melanocytes show global downregulation of adhesion pathways

(A) Western blot of EW2.1 and EW2.2 Cdc42 f/f; ROSA26::Cre-ER^{T2}; CDKN2^{-/-} primary melanocyte cell line lysates probed for Cdc42 and GAPDH (B) Principal component analysis (PCA) plot of the RNA sequencing data showing the trends exhibited by the expression profiles of Cdc42 KO in EW2.1 (red, KO1) and EW2.2 (pink, KO2) and wild-type EW2.1 (dark blue, WT1) and EW2.2 (light blue, WT2). Significant expression changes between KO and WT cell lines ($p_{adj} < 0.05$) were submitted to DAVID Gene Ontology analysis. (C) Significantly enriched KEGG Pathways ($pValue < 0.05$) for genes demonstrating an increase (Up) in expression. (D) Hierarchical clustering analysis of KEGG GO: 'Lysosome' genes identified as significantly changed in the Up dataset. Heat bar indicates the mean log₂ fold change in gene expression between KO and WT cell lines EW2.1 and 2.2. (E) Significantly enriched KEGG Pathways ($pValue < 0.05$) for genes demonstrating a decrease (Down) in expression. (F) Hierarchical clustering analysis of KEGG GO: 'Focal adhesion' genes identified as significantly changed in the Down dataset. Heat bar indicates the mean log₂ fold change in gene expression between KO and WT cell lines EW2.1 and EW2.2. (G) Western blot on EW1 and EW7 lysates probed for $\alpha 4$ integrin and α -tubulin. (H) Normalised integrated density of Western blot bands from three independent experiments. (I) EW1 and EW7 probed for $\beta 3$ integrin and α -tubulin. (J) Normalised integrated density of Western blot bands from three independent experiments. (K) Average RNA expression level of selected Rho-family GTPases in DMSO treated control melanocytes versus OHT treated Cdc42 f/f melanocytes, taken from global RNA-sequencing data (Supplemental Spreadsheet Table S1). Graphs show mean \pm SEM * $p < 0.05$, ** $p < 0.01$, t-test. *Linked to Figure 5.*

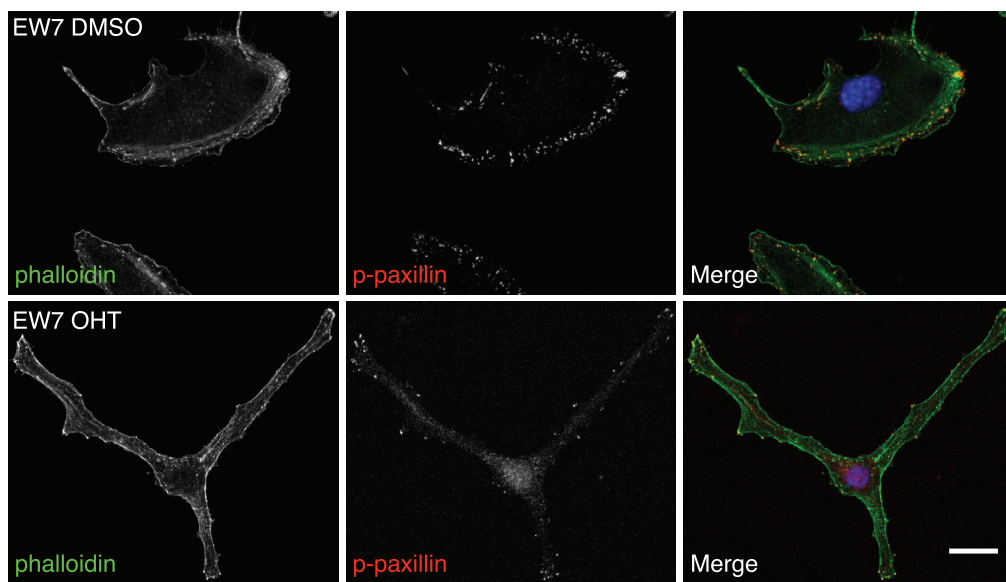
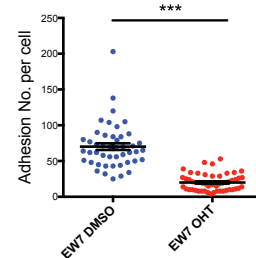
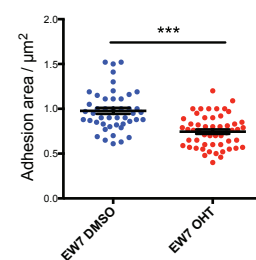
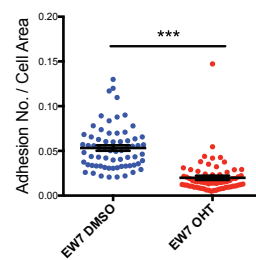
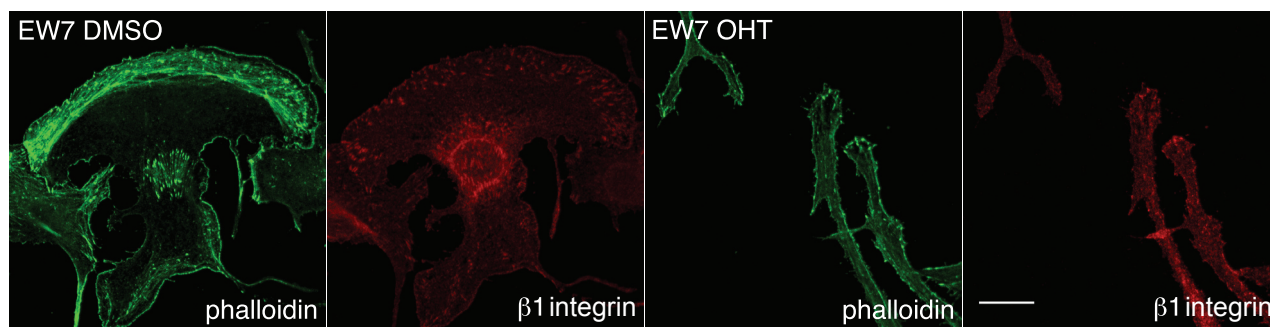
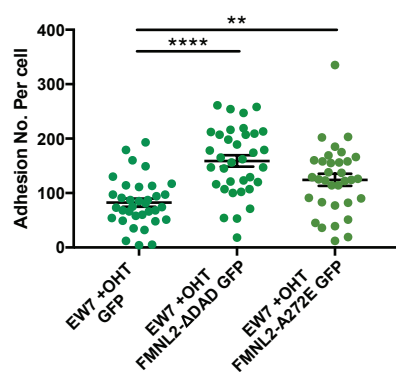
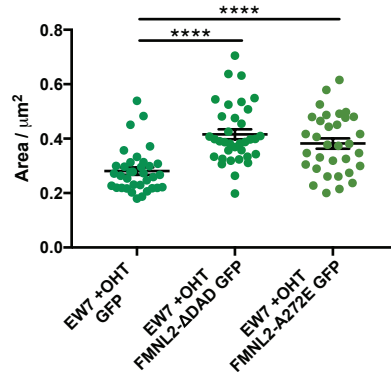
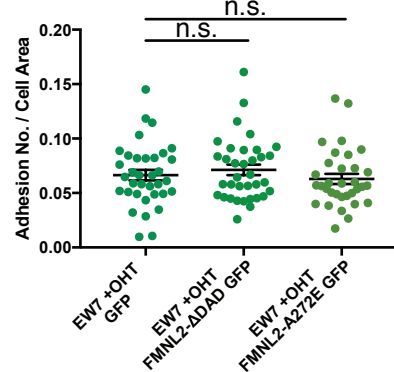
A**B****C****D****E****F****G****H**

Figure S6- Focal adhesions are reduced in Cdc42 null cells and partially restored by FMNL2

All panels show EW7 Cdc42 f/f; ROSA26::Cre-ER^{T2}; CDKN2^{-/-} melanocytes treated with DMSO (control) or OHT (to delete Cdc42). (A) Control and OHT-treated EW7 cells stained with Alexa-fluor 488-conjugated phalloidin (green) and anti-phospho-paxillin antibody (red). Scale 15µm. N ≥ 46 cells per condition over 3 experiments. Graphs show adhesion number per cell (B), adhesion area (C) and number of adhesions normalised to the cell area (D) were calculated using thresholded phospho-paxillin staining (E) Control or OHT-treated EW7 cells stained with Alexa-Fluor 488-conjugated phalloidin (green) or anti-β1 integrin antibody (red). Scale 15µm. (F-H) Bar graphs show data from OHT-treated EW7 transfected with GFP, FMNL2-ΔDAD-GFP or FMNL2-A272E-GFP fixed and stained with anti-vinculin antibody. Adhesion number per cell (F), adhesion area (G) and number of adhesions normalised to the cell area (H) were calculated using thresholded vinculin staining. N = 33-35 cells per condition over 3 experiments. Graphs show mean ± SEM, **p<0.01, ***p<0.001, ****p<0.0001, n.s. not significant, t-test with Welch's correction.

Linked to Figure 6

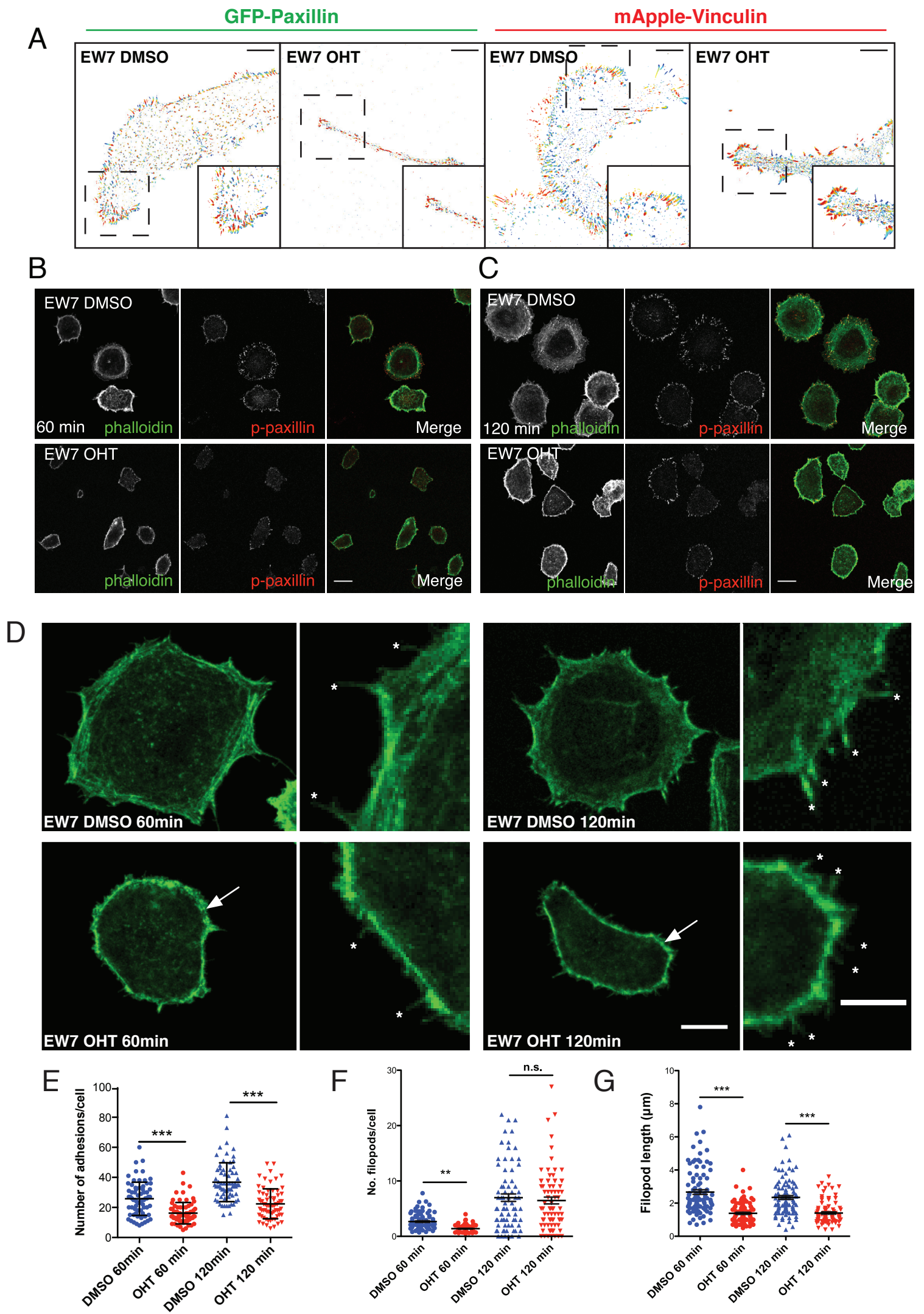


Figure S7

Figure S7- Cdc42 knockout melanocytes have altered adhesion and spreading dynamics

All panels show EW7 Cdc42 f/f; ROSA26::Cre-ER^{T2}; CDKN2^{-/-} melanocytes treated with DMSO (control) or OHT (to delete Cdc42). (A) Example images from Focal Adhesion Analysis Software [S13] quantification of adhesion dynamics in EW7 melanocytes, expressing GFP-paxillin or mApple-vinculin. Black box shows inset. Scale 10 μ m. (B-D) Control or OHT-treated EW7 melanocytes, stained with Alexa-fluor 488-conjugated phalloidin (F-actin, green), anti phospho-paxillin antibody (red) as indicated. Scale 15 μ m. (B) Cells after 60min of spreading (C) After 120min of spreading (D) After 60 or 120min of spreading. White asterisks indicate structures counted as filopod-like structures (FLS). White arrows indicate thick actin cortex. (E) Number of adhesions at 60min and 120min, N = 75 cells per condition over 3 experiments. (F) Number of FLS 60 or 120min after spreading. (G) FLS length per cell 60 or 120min after spreading. Line graph shows mean \pm SEM n.s. = not significant, **p<0.01, ***p<0.001, n.s. not significant, t-test with Welch's correction.

Linked to Figure 7

Supplemental Experimental Procedures

Mouse Strains and Genotyping

Cdc42 flox mice were previously described [S1]. Tyrosinase CreB mice [S2], Lifeact-mEGFP mice [S3] and CDKN2 locus deficient mice in C57BL6/J background were previously described [S4, S5]. LacZ/EGFP (Z/EG) mice [S6], DCT-LacZ (DCT::LacZ) [S7] mice in mixed background were previously described. ROSA26Cre::ERT2 mice were obtained from Dr David Adams at the Sanger Institute and previously described [S8]. No phenotype was observed from Cdc42 wt/wt; Tyr::CreB+ mice so these mice were also included in the control groups.

Antibodies, Cell Reagents and Constructs

Mouse anti-Cdc42, Mouse anti-GM130, Mouse anti-BrdU (for IHC), Mouse anti-ROCKII (BD Biosciences), Goat anti-DCT TRP2, Mouse anti-T-MLC MRCL3/MRCL2/MYL9 (E-4), Rabbit anti-WAVE2 (Santa Cruz), Mouse anti-Rac1 (Cytoskeleton), Mouse anti-vinculin (hVIN1, Sigma), Rabbit anti-Phospho-Myosin Light Chain 2 (Thr18/Ser19), Rabbit anti-Phospho Myosin Light Chain 2 (Ser19) for immunofluorescence (Cell Signalling Technology), Rabbit anti-phospho-paxillin, Rabbit anti-GAPDH, Rabbit anti- α 4 integrin for Western blots, Rabbit anti- β 3 integrin, Rabbit anti- α 6 integrin (Cell Signalling), Rabbit anti- α 4 integrin (D2E1, Cell Signalling Technology, for immunofluorescence) rabbit anti-Ki67 (SP6, Neomarkers), Mouse anti-BrdU (Dako), Rabbit anti-p34-Arc, Rat anti- β 1 integrin (Millipore), Mouse anti GAPDH (Ambion) Rabbit anti- α -Tubulin, Rat anti-tyrosinated tubulin, mouse anti-FMN2 antibody (Abcam) Mouse anti-Talin (8D4, Sigma), Sheep anti-MITF (kind gift of Claudia Wellbrock, Manchester University, UK). Monoclonal biotinylated rabbit anti-goat IgG secondary antibody was obtained from Dako. Rhodamine phalloidin, anti-mouse IgG, anti-rabbit IgG and anti-goat IgG AlexaFluor secondary antibodies were obtained from Life Technologies. Horseradish peroxidase-conjugated secondary (Cell Signalling).

Immunohistochemistry of Pup and Embryo Skin

Pup skin was shaved and dermal/epidermal skin layer was removed from the back and belly. Skin was stuck dermis-down onto Whatman paper then skin and paper were cut along the directions of hair growth. Strips were placed in formalin and left to fix overnight before embedding. These sections were stained exactly as previously described [S3]. To fluorescently stain embryo sections for proliferation, mothers were first injected with 2.5mg BrdU (BD Bioscience) at the desired embryonic day then embryos were harvested 2 or 24h after injection, dissected, washed in PBS and fixed overnight in formalin before histological processing. Embryos were cut transversely and embedded into blocks head or tail down. These sections were stained exactly as previously described [S3].

X-Gal staining of Embryos and Dermal/Epidermal Visualisation

Timed embryos were harvested and stained as described previously [S9, S10]. Briefly, Embryos were dissected in PBS and fixed in ice-cold 0.25% glutaraldehyde in PBS for 30 minutes. Embryos were washed for 10 minutes in ice-cold PBS, and placed in permeabilisation solution (2 mM MgCl₂, 0.01% sodium deoxycholate and 0.02% NP-40 in PBS) for 30 minutes at room temperature and stained with X-gal staining solution (2 mM MgCl₂, 0.01% sodium deoxycholate, 0.02% NP-40, 5 mM K₄Fe(CN)₆, 5 mM K₃Fe(CN)₆ and 1 mg/ml X-gal (Promega) in PBS) for 48 hours at 4°C. Embryos were stored in 10% formalin after washes with PBS. Embryo images for quantification were taken at the same magnifications with a Zeiss Stemi-2000 dissection microscope (EOS utility, Edmund Optics, NJ, USA). For imaging of the dermal/epidermal distribution of melanocytes, freshly stained embryos were sectioned transversely and embedded into paraffin blocks head or tail down. Sections were then counterstained with light eosin to reveal the skin structure.

Ex-vivo Skin Explant Imaging

Experimental set up was adapted from [S11]. E15.5 embryos were harvested and dissected, removing a section of the embryonic skin containing the dermis and epidermis. The sample was sandwiched between a nuclepore membrane (Whatman) and a gas permeable Lumox membrane in a 24-well Greiner Lumox culture dish so that the epidermal side of skin was in contact with Lumox membrane. Matrigel (BD Bioscience) was used to cover the membrane and the plate was incubated at 37°C for 10 min. Culture medium (Phenol red free DMEM supplemented with 10% FBS and 100 mg/ml primocin) (InvivoGen) was added. Time-lapse images were captured using an Olympus FV1000 or Nikon A1 confocal microscope in a 37°C chamber with 5% CO₂ for 4 hrs.

Analysis of Motility in Skin Explants

Pseudopods were defined as any type of protrusion extending outwards from the cell body. In melanoblasts these are the long thin extensions that the cells extend between surrounding keratinocytes. In some cases, additional pseudopods branched from an established pseudopod. In these cases, the nascent branched pseudopod was counted as a new pseudopod, with its own lifetime. The lifetime of a pseudopod was defined as the time that the pseudopod began to extend until its complete retraction back to its starting point.

Melanoblast Tracking in Ex-Vivo Skin Explants

Melanoblasts were tracked separately using the MTrackJ ImageJ plugin from time-lapse images taken every 5 minutes for 4 hours. Speed measurements were taken from these tracks produced by the MTrackJ plugin. At least 100 melanoblasts from at least three different skin explants from different embryos were quantified. Mean values \pm SEM and statistical analyses were calculated and plotted using Graphpad Prism (Graphpad Software) and significance was determined using two-tailed unpaired t-tests.

Melanocyte Isolation and Transfection

We created several cell lines from the embryos and in general they all behaved similarly. EW1, EW2.1, EW2.2 and EW7 were chosen for experiments as they grew the best and showed consistent behavior in culture. We performed most of our experiments with EW1 and EW7, but we were not able to grow these cells to a high enough density to isolate RNA to perform the RNA-seq analysis with them. We therefore used lines EW2.1 and EW2.2 for the RNA-seq analysis.

Melanocytes were isolated from 1 day old *Cdc42 f/f; ROSA26:Cre-ERT2;CDKN2^{-/-}* pups (EW1, EW7, EW2.1, EW2.2) according to methods already described [S3]. Contaminating fibroblasts and keratinocytes were removed by treatment with G418 (50 μ g/ml) for 4 days per week and extensive washing with PE (PBS+ 1mM EDTA). Pure cultures were obtained two months after isolation. Melanocytes were cultured in F-12 (Gibco) growth media containing 200nM Phorbol Myristate Acetate (PMA, Sigma) and 100 μ g/ml primocin (Invivogen) at 37°C with 5% CO₂ and passaged at 50% confluency. Melanocytes were passaged up to a maximum of 20 times. Cells were treated with DMSO or 1 μ M OHT for 5 days prior to use in assays, with media and drugs refreshed once. To transfect, 1x10⁴ cells were seeded into 6-well plates the day preceding transfection. Each well was transfected with 4 μ g of plasmid using 10 μ l of LipofectamineTM reagent (Invitrogen) according to the manufacturers instructions. Cells were then moved onto coverslips coated with 20 μ g/ml fibronectin from bovine plasma (Sigma) on the day prior to imaging (see live cell imaging methods).

Melanocyte Growth Assay

DMSO or OHT treated melanocytes as described were seeded into 6 well plates in triplicate. Cells were counted each day for 4 days using a haemocytometer. This was repeated 3 times.

Flow Cytometry and Cell Cycle Analysis

Pregnant mice were injected with 2.5mg BrdU 2 or 24hrs prior to harvesting of embryos and co-staining with DCT (Santa Cruz) and BrdU (DAKO) antibodies. For cell-cycle analysis, melanocytes were incubated for 3hrs with 10 μ M BrdU (BD bioscience) and fixed and stained as previously described [3]. Briefly, cells were fixed in 70% ethanol in suspension overnight at 4°C. Cells were then sedimented, washed and bleached using a melanin bleaching kit (Polysciences Inc) according to manufacturers instructions. Cells were then washed and re-suspended in 4N HCl for 15min then stained with mouse anti-BrdU (DAKO) in PBT (0.1% BSA, + 0.001% Tween in PBS) for 30min, then with Alexa-Fluor-488 conjugated goat anti-mouse secondary antibody in PBT for 30min. After washing, cells were stained in propidium iodide (1mg/ml) for 30min before analysis by BD FACS-Calibur (BD Bioscience).

Immunofluorescence

Cells were fixed in either 4% Paraformaldehyde for 20 minutes or -20°C methanol for 4 minutes, permeabilised for 3 minutes with 1% NP-40 in PBS permeabilisation buffer and blocked for 30 minutes using 10% goat serum in PBS. Primary antibodies were incubated for 1 hour in 1% goat serum. These were detected with species-specific Alexa488, Alexa594 and Alexa647-conjugated secondary antibodies (Life Technologies). Coverslips were then mounted in Prolong anti-fade mounting solution with DAPI (Thermo Fisher) and imaged using a Nikon A1 inverted laser scanning confocal microscope.

Live cell imaging

For imaging of melanocyte migration, cells were plated onto glass-bottom dishes coated with fibronectin from bovine plasma (Sigma) by incubation for 2 hours with 20 μ g/ml fibronectin in PBS followed by extensive PBS wash. Cells were seeded onto dishes the day prior to imaging. Time-lapse movies were acquired using a Nikon TE2000 microscope in a 37°C chamber with 5% CO₂.

Immunoblotting

DMSO and OHT treated melanocytes were lysed and scraped from dishes in RIPA buffer (50mM Tris-HCl, 150mM NaCl, 1% NP-40 and 0.25% Na-deoxycholate) with protease inhibitor cocktail (Thermo scientific) and phosphatase inhibitor cocktail (Thermo scientific) and left for 5 min on ice. Lysates were clarified by centrifugation at 15,000 rpm and separated by SDS-PAGE and transferred to PVDF membranes. Primary antibodies were detected with fluorescently conjugated secondary antibodies and detected by LI-COR imager. Images were processed used the LI-COR ImageStudioLite software.

Polarity measurement

Glass bottom dishes were coated with 20 μ g/ml of fibronectin and then Ibidi culture-inserts were placed in the dishes. Cells were then seeded into the inserts and left overnight at 37°C with 5% CO₂. The inserts were then removed, medium was added to the dishes and the cells were returned to the incubator for 3hrs. Immunofluorescence was performed with DAPI, Alexa-fluor 568-conjugated phalloidin and anti-GM130 antibody. Images were acquired using Olympus FV1000 confocal microscope with a PlanApo N 60x/1.4 oil objective. To analyse the polarity of cells, lines at a 120° angle representing the front 1/3 and rear 2/3 of the cell area were placed over the nucleus of all of the cells in the field of view. Polarised cells were defined as cells where the Golgi resided in at least 50% of the area facing the direction of movement. To analyse the distribution of Golgi throughout each cell, it was determined if the Golgi was spread out over 1, 2 or all 3 of the sections formed by the lines at 120°.

Rescue with α 4 integrin

OHT treated EW7 melanocytes were co-transfected with eGFP-C1 (empty vector) and pcDNA3.1 (control), or eGFP-C1 and pcDNA3.1- α 4 integrin wt (human, Addgene plasmid # 80016, gift from Chinten James Lim). Melanocytes were seeded onto fibronectin-coated glass-bottom dishes for 24-hours, fixed and stained with anti- α 4 integrin and anti-vinculin antibodies. Cells were imaged with a Zeiss 880 LSM with Airyscan, with a Plan-Apochromat 40x/1.3 oil DIC M27 or Plan-Apochromat 63x/1.4 oil DIC M27 objective. Length to width ratio and cell Roundness were calculated using Image J (version 1.49o).

FMNL2 rescue and quantification

DMSO and OHT treated EW7 melanocytes were transfected with eGFP-N1 (empty vector), FMNL2-GFP, FMNL2- Δ DAD-GFP or FMNL2-A272E-GFP. FMNL2 constructs were constructed by FK and a gift from Prof. Klemens Rottner, Helmholtz Centre for Infection Research, Braunschweig, Germany. C-terminally tagged FMNL2-EGFP (NM_052905.3; residues 1-1092; isoform b) was as described [S12]. FMNL2 Δ DAD-EGFP (1-1026 aa) was generated by isolation of the insert sequence from EGFP-FMNL2 Δ DAD [12] using restriction enzymes Sall and SacII and subsequent ligation into an EGFP-N1 vector (Clontech Inc. Mountain View, CA, USA) using the same restriction sites. Constitutively active FMNL2-A272E-EGFP will be characterized elsewhere (Kage et al., unpublished), and was generated using Qiagen site directed mutagenesis kit employing forward primer 5'-GTCTTAGAACTGTTGGCAGAGGTTGTCTTGTCAGAGGCG-3' and the respective complementary sequence as reverse primer. Melanocytes were seeded onto fibronectin-coated glass-bottom dishes for 24-hours, fixed and stained with rhodamine-conjugated phalloidin. Cells were imaged with a Zeiss 880 LSM with Airyscan, with a Plan-Apochromat 40x/1.3 oil DIC M27 or Plan-Apochromat 63x/1.4 oil DIC M27 objective. Length to width ratio and cell Roundness were calculated using Image J (version 1.49o).

pMLC staining and quantification

DMSO and OHT treated melanocytes were transfected with eGFP-C1 (empty vector), seeded onto fibronectin-coated glass bottom dishes for 24-hours, fixed and stained with anti-pMLC S19 antibody and DAPI to stain nuclei. To quantify the intensity profile of pMLC staining using ImageJ (version 1.49o), a 10 μ m tall region of interest (ROI) was drawn starting at the centre of the nucleus and ending at the leading edge of the cell. The mean fluorescence intensity for each cell in all 3 channels (pMLC S19, GFP, DAPI) was determined using 'Plot Profile'. For each cell, these intensity values were

binned by percentile distance from the cell centre, i.e. 100 bins arranged from the nucleus to the cell edge, and the mean intensity for each bin was calculated (script written in Python version 3.5). Graphs show the mean shape taken by this profile across $N = 36-43$ cells over 3 biological repeats, with error bars showing the SEM.

Blebbistatin washout

Glass coverslips were coated with 20 μ g/ml of fibronectin and cells were seeded onto the coverslips overnight in an incubator at 37°C with 5% CO₂. Cells were then treated with a final concentration of 10 μ M Blebbistatin for 30 minutes, followed by either cell fixation or replacement of the medium with no Blebbistatin for 1 hr. Immunofluorescence was carried out using Alexa-fluor 568-conjugated phalloidin. Images of cells were acquired using Olympus FV1000 confocal microscope with a PlanApo N 60x/1.4 oil objective. Cell lengths and widths were measured using ImageJ.

Active-Rac pulldown assay

Active Rac levels were assayed using the kit from Cytoskeleton Inc, (Cat. # BK035). All manipulations were performed in a 4°C cold room and on ice where possible. Briefly, cells were lysed using PBD lysis buffer with appropriate protease inhibitor provided with the kit and clarified for a minute at 10000g/4°C. Equivalent amount of clarified lysates from control and OHT treated cells were loaded into 30 μ g of PBD beads and incubated at 4°C on a rotator for an hour. Beads were washed twice with 500 μ l wash buffer. 2x SDS buffer was added to each sample and boiled for 1 minute. Immunoblotting for Rac was performed using anti-Rac monoclonal antibody provided with the kit. Relative active Rac levels were quantified by setting control Rac-GTP levels to 100%. Mean and standard deviation shown from four repeats.

Quantifying Adhesion dynamics

For adhesion dynamics quantification, melanocytes were transfected with GFP-Paxillin or mApple-Vinculin-N-21 (Addgene Plasmid no. # 54962, gift from Michael Davidson), replated on fibronectin and imaged 24 hours later. Live-cell imaging was performed using a Zeiss 880 Laser Scanning Microscope with Airyscan at 37°C/5% CO₂ with a Plan-Apochromat 63x/1.4 oil DIC M27 objective. Cells were imaged for 30 minutes at 1-minute intervals using the 488nm or 561nm laser respectively. Movies were processed and exported using ZEN software (version 2.1 SP1 (black)). x/y drift was corrected using the Image Stabilizer plugin (K. Li, "The image stabilizer plugin for ImageJ," http://www.cs.cmu.edu/~kangli/code/Image_Stabilizer.html, February, 2008) for Fiji/Image J (version 1.49o) prior to analysis.

Movies were submitted to the Focal Adhesion Analysis Server (FAAS) [S13] for analysis of adhesion dynamics. The mean rate of adhesion assembly/disassembly was calculated for each cell ($N = 15$ cells per condition over 3 independent experiments).

RNA Isolation and quality check

RNA for sequencing was isolated from two melanocyte cell lines (EW2.1 and 2.2) that had been pre-treated with DMSO or OHT for 5 days. RNA was isolated using the RNeasy isolation kit from Qiagen according to the manufacturers instructions. The concentration of the RNA sample was estimated using the NanoDrop system (Thermo scientific) and was kept at -80°C for long-term storage. The quality of the RNA was checked using the 4200 Tapestation from Agilent technologies, and deemed of suitable quality to perform sequencing.

RNA Sequencing and analysis

The RNA library was prepared using the Library Prep kit (Illumina TruSeq RNA Sample prep kit v2) according to methods previously described [S14]. Libraries were sequenced using the Illumina NextSeq500 platform using the sequencing Kit High Output v2 75cycles (2x36cycle Paired End, single index). Quality checks on the raw RNASeq data files were done using fastqc (<http://www.bioinformatics.bsrc.ac.uk/projects/fastqc>) and fastq screen (http://www.bioinformatics.babraham.ac.uk/projects/fastq_screen/). RNASeq reads were aligned to the GRCm38 [S15] version of the mouse genome using tophat2 version 2.0.10 [S16] with Bowtie version 2.1.0 [S17]. Expression levels were determined and statistically analysed by a combination of HTSeq version 0.5.4p3 (<http://www-huber.embl.de/users/anders/HTSeq/doc/overview.html>), the R 3.1.1 environment, utilizing packages from the Bioconductor data analysis suite and differential gene expression analysis based on a generalized linear model using the DESeq2 [S18]. Significantly changed genes ($padj < 0.05$) were submitted to DAVID for Gene Ontology (GO) analysis [S19]. KEGG

Pathway analysis was performed for genes demonstrating an increase (Up) or decrease (Down) in RNA expression between KO and WT cell lines. Significant KEGG GO Terms were identified ($pValue < 0.05$, Supplemental spreadsheet). Hierarchical clustering of \log_2 fold changes in gene expression was performed on the basis of Euclidian Distance using complete linkage and visualised using MultiExperiment Viewer (MeV v4.8).

Adhesion Quantification

To quantify adhesion size and number, melanocytes pre-treated with DMSO or OHT for 5 days were seeded onto coverslips coated with 20 μ g/ml fibronectin the day prior to fixation. The following day, cells were fixed with 4% PFA and stained with anti-phospho-paxillin (Y118) or anti-vinculin antibody, and rhodamine-conjugated phalloidin according to the immunofluorescence protocol described above. Adhesions were quantified using the 'Analyse Particles' function in ImageJ software. Cells were selected one at a time using the selection tool. A standard threshold was applied to the cell, picking out individual adhesions. Next, the ImageJ binary 'Watershed' filter was applied to the image to separate areas joined by only one or two pixels, helping to separate adjacent adhesions. The 'Analyse Particles' function was then applied to count the number of adhesions per cell and the area of each adhesion. The results generated from this analysis were compared with some test quantifications done by hand to ensure accuracy. Cells taken from three independent experiments, at least 46 cells per genotype.

Spreading Assays

DMSO or OHT treated melanocytes were seeded onto 20 μ g/ml fibronectin, 10 μ g/ml Laminin-111 (Sigma) or 10 μ g/ml Concanavalin A (Sigma) and imaged at 15-minute intervals for 2-hours using a Nikon TE2000 microscope at 37°C/5% CO₂ using a 20x/0.45 S Plan Fluor objective. The area of attached cells at 15, 30, 60 and 120-minutes was quantified using the ImageJ selection tool and the 'Measure' function.' At least 89 cells from three independent experiments were quantified.

FLIM

To investigate the levels of active Rac in melanocytes, a dual-chain Rac1 biosensor (Rac1 FLARE.dclg) was used. This Rac1 FLARE biosensor was a kind gift from the Hahn lab (UNC Chapel Hill) and is a modification of the dual chain biosensor previously described in Machacek et al [S20]. CyPet was replaced by Turquoise fluorescent protein [S21] to improve brightness and FRET efficiency. The two biosensor chains were expressed on one open reading frame with two consecutive 2A viral peptide sequences from porcine teschovirus-1 (P2A) and Thosea asigna virus (T2A) inserted between them, leading to cleavage of the two chains during translation [S22]. The detailed characterisation of this new probe will be described elsewhere.

The biosensor construct or the control dTurquoise construct was transfected into melanocytes. The following day, they were moved onto 35mm glass bottom dishes (MatTek corporation) coated with 20 μ g/ml fibronectin for FRET imaging the following day. Probe lifetime was measured on a whole cell basis using the Nikon FLIM/TIRF system Z6014 and analysed through the LI-FLIM software.

Supplemental References

- S1. Czuchra, A., Wu, X., Meyer, H., van Hengel, J., Schroeder, T., Geffers, R., Rottner, K., and Brakebusch, C. (2005). Cdc42 is not essential for filopodium formation, directed migration, cell polarization, and mitosis in fibroblastoid cells. *Mol Biol Cell* 16, 4473-4484.
- S2. Delmas, V., Martinozzi, S., Bourgeois, Y., Holzenberger, M., and Larue, L. (2003). Cre-mediated recombination in the skin melanocyte lineage. *Genesis* 36, 73-80.
- S3. Li, A., Ma, Y., Yu, X., Mort, R.L., Lindsay, C.R., Stevenson, D., Strathdee, D., Insall, R.H., Chernoff, J., Snapper, S.B., et al. (2011). Rac1 drives melanoblast organization during mouse development by orchestrating pseudopod-driven motility and cell-cycle progression. *Dev Cell* 21, 722-734.
- S4. Ackermann, J., Fruttschi, M., Kaloulis, K., McKee, T., Trumpp, A., and Beermann, F. (2005). Metastasizing melanoma formation caused by expression of activated N-RasQ61K on an INK4a-deficient background. *Cancer Res* 65, 4005-4011.
- S5. Serrano, M., Lee, H., Chin, L., Cordon-Cardo, C., Beach, D., and DePinho, R.A. (1996). Role of the INK4a locus in tumor suppression and cell mortality. *Cell* 85, 27-37.
- S6. Novak, A., Guo, C., Yang, W., Nagy, A., and Lobe, C.G. (2000). Z/EG, a double reporter mouse line that expresses enhanced green fluorescent protein upon Cre-mediated excision. *Genesis* 28, 147-155.

- S7. Mackenzie, M.A., Jordan, S.A., Budd, P.S., and Jackson, I.J. (1997). Activation of the receptor tyrosine kinase Kit is required for the proliferation of melanoblasts in the mouse embryo. *Dev Biol* *192*, 99-107.
- S8. Hameyer, D., Loonstra, A., Eshkind, L., Schmitt, S., Antunes, C., Groen, A., Bindels, E., Jonkers, J., Krimpenfort, P., Meuwissen, R., et al. (2007). Toxicity of ligand-dependent Cre recombinases and generation of a conditional Cre deleter mouse allowing mosaic recombination in peripheral tissues. *Physiol Genomics* *31*, 32-41.
- S9. Loughna, S., and Henderson, D. (2007). Methodologies for staining and visualisation of beta-galactosidase in mouse embryos and tissues. *Methods Mol Biol* *411*, 1-11.
- S10. Li, A., and Machesky, L.M. (2013). Rac1 cycling fast in melanoma with P29S. *Pigment Cell Melanoma Res*.
- S11. Mort, R.L., Hay, L., and Jackson, I.J. (2010). Ex vivo live imaging of melanoblast migration in embryonic mouse skin. *Pigment Cell Melanoma Res* *23*, 299-301.
- S12. Block, J., Breitsprecher, D., Kuhn, S., Winterhoff, M., Kage, F., Geffers, R., Duwe, P., Rohn, J.L., Baum, B., Brakebusch, C., et al. (2012). FMNL2 drives actin-based protrusion and migration downstream of Cdc42. *Curr Biol* *22*, 1005-1012.
- S13. Berginski, M.E., and Gomez, S.M. (2013). The Focal Adhesion Analysis Server: a web tool for analyzing focal adhesion dynamics. *F1000Res* *2*, 68.
- S14. Fisher, S., Barry, A., Abreu, J., Minie, B., Nolan, J., Delorey, T.M., Young, G., Fennell, T.J., Allen, A., Ambrogio, L., et al. (2011). A scalable, fully automated process for construction of sequence-ready human exome targeted capture libraries. *Genome Biol* *12*, R1.
- S15. Church, D.M., Schneider, V.A., Graves, T., Auger, K., Cunningham, F., Bouk, N., Chen, H.C., Agarwala, R., McLaren, W.M., Ritchie, G.R., et al. (2011). Modernizing reference genome assemblies. *PLoS Biol* *9*, e1001091.
- S16. Kim, D., Pertea, G., Trapnell, C., Pimentel, H., Kelley, R., and Salzberg, S.L. (2013). TopHat2: accurate alignment of transcriptomes in the presence of insertions, deletions and gene fusions. *Genome Biol* *14*, R36.
- S17. Langmead, B., and Salzberg, S.L. (2012). Fast gapped-read alignment with Bowtie 2. *Nat Methods* *9*, 357-359.
- S18. Love, M.I., Huber, W., and Anders, S. (2014). Moderated estimation of fold change and dispersion for RNA-seq data with DESeq2. *Genome Biol* *15*, 550.
- S19. Huang da, W., Sherman, B.T., and Lempicki, R.A. (2009). Systematic and integrative analysis of large gene lists using DAVID bioinformatics resources. *Nat Protoc* *4*, 44-57.
- S20. Machacek, M., Hodgson, L., Welch, C., Elliott, H., Pertz, O., Nalbant, P., Abell, A., Johnson, G.L., Hahn, K.M., and Danuser, G. (2009). Coordination of Rho GTPase activities during cell protrusion. *Nature* *461*, 99-103.
- S21. Goedhart, J., van Weeren, L., Hink, M.A., Vischer, N.O., Jalink, K., and Gadella, T.W., Jr. (2010). Bright cyan fluorescent protein variants identified by fluorescence lifetime screening. *Nat Methods* *7*, 137-139.
- S22. Kim, J.H., Lee, S.R., Li, L.H., Park, H.J., Park, J.H., Lee, K.Y., Kim, M.K., Shin, B.A., and Choi, S.Y. (2011). High cleavage efficiency of a 2A peptide derived from porcine teschovirus-1 in human cell lines, zebrafish and mice. *PLoS One* *6*, e18556.